

This resulted in a horizontal position accuracy of 2–5 m. The vertical accuracy of the Atlas DS3 hydrosweep multibeam system was better than 0.2 % of the water depth according to the manufacturer's specification.

During post-processing with the hydrographic software package Caris Hips & Sips[®] 8.0, the multibeam data were cleaned for artefacts related to erroneous calibration values, spurious soundings, vessel motion, navigational jumps, and sound velocity refractions. Sound velocity corrections were applied to the data based on sound velocity profiles calculated from CTD data using the approach by Chen and Millero (1977). In addition, the pre-processed data were imported in the editing and visualization software package QPS Fledermaus[®] for area-based editing.

2.1.2 DTM generation

From the cleaned swath bathymetry data sets, a digital terrain model (DTM) was created (Fig. 1). Gaps in the multibeam coverage of Nachtigaller Hill were filled and interpolated on the basis of the IBCSO grid (Arndt et al., 2013). By applying a “remove-and-restore techniques” (Arndt et al., 2013; Jakobsson et al., 2000, 2008, 2012). Horizontal resolutions were 10 m for areas with multibeam coverage recorded during our cruise, 500 m for areas previously mapped and 2000 m for areas where the bathymetry was derived from the General Bathymetric Chart of the Ocean (GEBCO) and satellite altimetry. For a better consistency of the DTM and to minimise artefacts arising from the use of various data source, an integration (bending) algorithm (Arndt et al., 2013) was applied. The final DTM was projected to UTM Zone 21S with a datum of WGS1984. For all subsequent analyses raster data sets were derived from this DTM.

2.2 Geo-statistical analyses

Geo-statistical analyses were performed with the ESRI[®] in ArcGIS[®] software package including the toolbox extensions Benthic Terrain Modeller (BTM) (Wright et al., 2005) and the LandSerf software (Wood, 2009a). In both software packages, raster

1637

analyses were performed at a number of scales following a trial-and-error approach to find the best representation of the different geo-morphological features encountered at the Nachtigaller Hill. For consistency, these analyses were limited to the areas with high-resolution (10 m) multibeam coverage and the shallow parts of the hill (Fig. 1). To further reduce the influence of potential artefacts from outer beams of the multibeam sonar swath, the outer 50 m of the multibeam coverage and hill area were ignored in all geo-statistical analyses

For visual inspections, and for a more natural representation of the bathymetric data, hillshade images were calculated in ArcGIS[®]. Hillshade images provide an illuminated, pseudo-3-D impression that allows for the identification of small morphological structures that were otherwise unrecognisable in the bathymetry data. In addition, slope (the first derivative of the topography) and ruggedness (a second derivative of the topography) were calculated as topographic terrain descriptors. Slope calculation were performed in ArcGIS[®] applying the equation described in Burrough and McDonnell (1998). Ruggedness was calculated with the LandSerf software (Wood, 2009a) from a bivariate quadratic approximated terrain surface (Wood, 2009b) and is measure for the roughness or “bumpiness” of the seabed (Wilson et al., 2007). For more advanced geo-statistical analyses, a focal statistic approach was applied. Both, broad-scale and fine-scale Bathymetric Position Index (BPI) grids were calculated using the BTM extension version 3.0 (beta) for ArcGIS 10.1 (Wright et al., 2005). The BPI represents a marine equivalent of the topographic position index commonly used in terrestrial landscape studies (Lundblad et al., 2006; Weiss, 2001) and is a second-order derivative of the bathymetry (Guinan et al., 2009). It calculates the depth differences between each bathymetric raster cell and the average depth of a surrounding reference area (in this study an annulus-shaped area). Consequently, cells with positive BPI values represent parts of elevated features or convex seabed, while cells with negative BPI values belong to depressions or concave seabed. BPI raster were used for geo-morphological analyses and for a seabed classification with the BTM (Wright et al., 2005). The BTM comprises a set of algorithms designed for seabed classifications solely on the basis

1638

of bathymetric data and bathymetry derivatives (Erdey-Heydorn, 2008; Lundblad et al., 2006; Weiss, 2001; Wright et al., 2005). The BPI raster formed the backbone of the classification. For the BTM, broad-scale and fine-scale BPI raster were computed. For these BPIs, the sizes of the reference areas were selected on the basis of trial-and-error decisions. Eventually, for the broad (fine) BPI an inner radius of 1000 m (30 m) and an outer radius of 1500 m (50 m) were chosen. With these parameters, the overall shape of the hill, its plateau, slopes, terraces and the background seabed, were well captured. The fine BPI raster highlighted local feature such as iceberg scours and escarpments. To avoid the influence of spatial auto-correlation in the broad and fine scale BPIs, the BPIs were standardised relative to 1 standard deviation each (Wright et al., 2005). The BTM furthermore requires a classification table to define a classification scheme. In this study, a modified version of the classification table of Erdey-Heydorn (2008) and Wienberg et al. (2013) provided the best results (Table 1).

2.3 Seabed imagery

Seabed imaging surveys were carried out with the Ocean Floor Observation System (OFOS) of the AWI deep-sea group. OFOS is a surface-powered, deep-towed gear equipped with a high-resolution (21 MPix), wide-angle CANON EOS 1Ds Mark III camera system. Towed behind the ship at a speed of 0.5 kn, OFOS was operated at a preferred height of 1.5 m above the seabed. The recorded high-resolution vertical seabed images show on average an area of 4.76 m^2 ($\sigma = 2.49 \text{ m}^2$). Three 50 cm spaced laser markers provided a scale in each photo. OFOS had two modes of operation. In automatic mode, a seabed photograph was taken every 30 s along the transects. With a ship speed of 0.5 kn, the average distance between the seabed images was approximately 8 m. In addition to the automatic mode, the camera was triggered manually, when the vertical ship's movement caused high variation of the height of the camera above the bottom (and consequently high variation in the area covered per image) and to record additional images from sites or organisms of specific interest.

1639

In total, 1875 seabed photographs were taken along four transects on the north-eastern side of Nachtigaller Hill. Together, the photographs depicted more than 8900 m^2 of seafloor. All transects were run downslope in south–north-direction. The westernmost transect (185-1, Fig. 1) ranged from 36 mwd to 397 mwd and covered parts of the plateau and almost the entire slope along a distance of 4287 m. Transect 189 (Fig. 1) was 1095 m long and covered only the upper slope between 29 and 186 m wd. The two easternmost transects (186-1 and 188-1, Fig. 1) partly overlapped and were combined 8224 m long. They ranged from 31 mwd on top of the hill, across the slope and the hill foot onto the background shelf at 413 mwd (Fig. 1). Images that were taken too close to or too far away from the seabed were discarded from the analyses. To identify these pictures, the seabed footprint of each image was calculated, using the opening angle of the camera and its altitude above the seabed. After discarding the lower and upper 5-percentile of images closest and furthest from the seabed, a total of 1730 stills remained for the seabed image analyses.

2.4 Seabed image analyses

From each photograph, environmental and biological parameters were analysed. Due to the relevance of hard substrate for benthic species distribution, the abundances of ice rafted detritus (IRD) (i.e. boulders and pebbles), were semi-quantitatively assessed using the following categories: single boulders or gravel, boulder or gravel coverage of less than 10 %, 10–30 %, 30–50 %, 50–70 %, 70–90 % and more than 90 %. IRD is the main source of hard substrate in the study area. It is furthermore a potential proxy for the strength of bottom currents and, hence, advective food supply. In addition, broken-up outcropping rocks were mapped as hard substrate, but also as proxy for erosion processes that are, in turn, also indicators of enhanced bottom currents. Soft substrate was categorised into sand and consolidated and soft fine sediment. The occurrence of sand (often with ripple structures) was regarded as evidence of winnowing and enhanced energetic regimes. Exposed consolidated sediments represented intermediate substrate (neither hard nor soft substrate) capable of forming steep cliffs and escarp-

1640

ments. Information on bioturbation and erosion processes was qualitatively extracted from the images (Fig. 3). Bioturbation represented intense burrowing in soft sediments. Ripples, only identified in sandy substrate, were indicative of lateral sediment transport and, thus, enhanced bottom currents. Erosion features and escarpments were proxies for enhanced bottom currents undercutting successions and forming cliffs. Trails of coarse sediments behind obstacles provided an additional proxy for moderately enhanced bottom currents. Striations on the seabed marked the impacts and scouring of icebergs (Figs. 3 and 4). Heavily bioturbated soft sediments on the foot of the hill and in the adjacent areas represented the background sedimentation.

For the biological analyses, the occurrences of the most abundant higher taxa (encrusting red algae, erected red algae, brown algae, sponges, hydrozoans, solitary ascidians, compound ascidians, gorgonarians, bryozoans and ophiuroids) were semi-quantitatively assessed. For each seabed image, the seafloor cover of these taxa was estimated, serving as a gross proxy for biomass. Abundance categories were “absent”, 1–5 %, 6–30 % and >30 % cover. Ophiuroids were categorised into “absent”, 10, 11–100 and >100 individuals per image, assuming that this abundance measure corresponds best with the seafloor-cover of the sessile taxa. In addition, the number of animal phyla in each image was categorised into three classes (1–3 phyla, 4–8 phyla and >8 phyla per image) representing a gross indicator for overall biodiversity. In addition, also the presence of brownish benthic diatoms films on the sediment surface and the occurrence of very high abundances of suprabenthic krill (>200 individuals per image) were recorded. All results from the seabed image analyses were geo-referenced and included in the GIS to generate maps of the relevant proxies and parameters (Fig. 5).

2.5 Biostatistical analyses

Correlations between biological and environmental data were calculated using the BIOENV routine of the statistical package PRIMER (Clarke and Gorley, 2006). Similarities between images were calculated for both the biological data (using the Bray–Curtis index) and the environmental variables (after normalisation; using the Euclidean

1641

distance). The strength of the relationship between the biotic and environmental patterns was quantified with a Spearman rank correlation coefficient between all (chosen) biological parameters (taxa) and any number and combination of environmental parameters. The BIOENV computations were performed for any of the following combination of approaches:

1. for similarities based on (1) single photographs (representative of a 10 m scale) and (2) averages of groups of 10 adjacent photographs (representative of a 100 m scale).
2. for similarities based on (1) all photographs of single stations, (2) all photographs of the stations 186 and 188 combined (because they represent a continuous transect) and (3) all photographs of all four stations combined in one data set.
3. for similarities based on the (1) biomass proxies for all high taxa, (2) number-of-phyla classes.

Prior to the similarity calculations, data were transformed in cases of skewed distribution of values for environmental parameters. A square-root transformation was applied in case of IRD and log transformations in case of slope and seabed ruggedness. Environmental parameters without a standard deviation (only photographs with exclusively zero values within one data set) were eliminated from BIOENV computations.

The influence of the seabed terrain, expressed through the qualitative BTM classification scheme (Table 1), on the composition of the epibenthos, determined through the semi-quantitative (0–3 scale) abundances of the most common higher taxa (see 2.6), was investigated by plotting the relative proportions of the selected taxa averaged within each BTM class. Moreover, within-BTM averages of the abundance of each selected taxon were computed and plotted to analyse potential distribution preferences of the taxa for certain BTM types.

3.3.3 Biology

With the exception of the shallowest quarter, transect 188 covered the hill foot and background shelf surroundings with a moderate number of phyla (Fig. 5d). Abundances of all animal taxa are generally lower than at the slope. Only ophiuroids show moderate abundances at the deepest part of transect 185 and occasionally at transect 188 (Fig. 5k). Sponges are generally characterized by moderate seabed coverages on single photos taken at the deepest section of the transects (Fig. 5e). Like solitary ascidians and gorgonians they are also absent from several images at the hill foot and shelf setting. In contrast, ophiuroids hydrozoans and compound ascidians are present in almost all images. A few photographs show high abundance of krill swimming close to the seabed at depths between 373 mwd and 385 mwd (Fig. 5l).

3.4 Biostatistics

The best and second best correlation results for all 24 parameter combinations (see materials and methods) for each run are listed in Table 2. Some of these correlations were moderate ($\rho = 0.5-0.722$), some were only poor ($\rho < 0.5$). For most of the individual computations, the ranking of correlations show no discrete step between “moderate” and “poor” correlations. Instead, the values for the correlation coefficient decrease continuously. Furthermore, the results differ considerably among the different approaches used (single photographs, averages of bins of 10 successive photographs, diversity and community approach). Since no clear result was obtained, an overarching analysis for the transects (186 and 188 considered as one transect) was conducted for the community approach. Only runs yielding correlation coefficients >0.5 were considered. All environmental factors were counted that contributed to these results within the single approaches.

Biotic distribution patterns are best explained by the abundance of IRD, followed by water depth. The parameters “escarpment”, “current”, “ruggedness” and “seabed classification” are never among any of the two best correlations. All remaining envi-

1647

ronmental parameters show only poor relationships to the distribution pattern in the biological data.

In case of the computations based on the number-of-phyla (diversity approach), the correlation coefficients of all individual results are too small to be used as a basis for a further comprehensive analysis. Alternatively, data were pooled for all images, independently of the transect. Results with a correlation coefficient >0.5 were only obtained for 10-binned photograph runs. These calculations returned better correlations for biological seafloor cover (or proxy) than for the number of phyla. The relevant environmental factors of both approaches are, however, similar. IRD, consolidated sediment, striated seabed (iceberg scouring) and ripples are relevant in all of the four computations. Sand and slope are relevant in 3 computations, and soft sediment, depth, slope, and ruggedness in only ≤ 2 runs.

The influence of the seabed terrain on the abundance and composition of the epibenthos was investigated for the six most frequent BTM classes (1, 2, 3, 8, 10, and 12; see Table 1 for explanation). Between 87 and 800 seabed photographs were designated to the individual BTM classes. BTM classes with lower frequencies were assumed to provide spurious results and, hence, excluded. The bar chart of the relative abundance proportions of the most abundant higher taxa averaged within each selected BTM class (Fig. 6a) shows that epibenthic composition did not differ much between the terrain types, except for BTM class 8 (Flat Top Ridges) where algae were abundant while they were rare or absent in the other BTM classes. The compound bar chart of the within-BTM averages abundances of the epibenthic taxa (Fig. 6b) also indicates the pronounced preference of algae for BTM class 8, since this terrain type was confined to the shallow plateau where enough sunlight can penetrate to the seabed to allow for the occurrence of primary producers. In contrast, the other epibenthic taxa were recorded with higher abundances in the other five selected BTM classes, a pattern that is evident for the most abundant taxa, hydrozoans and ophiuroids. These taxa reached highest densities in photos depicting “steep slopes” (BTM class 3) and at “local ridges, boulders, pinnacles on slopes” (BTM class 12).

1648

off Snow Hill and Dundee Island. Studies from the Larsen A shelf ice area have also shown that these sponges can recruit fast (Gutt et al., 2011 and references therein).

5 Typical high-latitude gorgonians (e.g. the genera *Thouarella* and *Dasystenella*) are distributed similarly. As a consequence, the epibenthos communities on the Nachtigaller Hill resemble those living along both sides of the Antarctic Peninsula rather than those found in the Eastern Weddell Sea. In this case, (short-distance) dispersal between Nachtigaller Hill and the Antarctic Peninsula must have happened perpendicular to the prevalent current from the south. Nachtigaller Hill is however located in the extension of the Antarctic Sound. This could facilitate recruitment with larvae from the western side of the Antarctic Peninsula. Larval drift, from the South-Eastern and Southern Weddell Sea must have happened over a longer distance with the Weddell Gyre.

4.2 Habitat distribution characterisation and distribution

15 Seabed classes, substrate types and benthic communities are crucial for defining benthic habitats (Dolan et al., 2008; Wienberg et al., 2008). Additional factors that control habitats are light penetration (depth of the photic zone), disturbance (iceberg scouring and slope collapse) (e.g. Gutt, 2000), bottom currents and the availability of nutrients. The first two factors can be derived from bathymetric seabed image data. Light levels are a function of the water depth and turbidity and, in polar regions, also of ice cover. In addition, the presence of macroalgae can be used to indicate the light level critical for photosynthesis. With regards to disturbance, iceberg scouring is the dominant process on the upper slope (although also deeper iceberg scours occur in the study area). Seabed traces of disturbances and erosion cannot always be linked to a specific process but coarse scour tails associated with boulder size IRD (Fig. 3) suggest that bottom currents can be at least temporarily erosive. Nutrient levels are another important factor for habitat characterisation. Unfortunately, no direct nutrient measurements are available for this study. However, the enhanced number of animal phyla and organism abundances on the hill slope (Fig. 5) is likely to indicate areas of enhanced nutrient levels.

1651

5 The results from analyses of the terrain (Fig. 2) and the seabed imagery (Fig. 4) both show that, in addition to the broad depth-related classification of the site in plateau, upper slope, foot and background setting, the hill is highly complex in terms of small-scale geo-morphology, seabed classes, substrate and benthic communities distribution. This complexity is captured in the seabed classification due to the incorporation of the fine scale BPI in the BTM.

10 In terms of habitat characterisation, the plateau is completely in the photic zone, hence the presence of macroalgae and diatom layers (Fig. 5). The overlying water mass is well mixed and homogenous. It, however, did not have a typical warm surface layer during the investigations in the middle of the austral summer (Fig. 6). Due to the shallow water depth, the impact of iceberg scouring is the dominant control on habitat distribution. Thus, the strongest contrast is between elevations exposed to frequent iceberg scouring and areas sheltered by elevations and ridges. In addition, wave action is another disturbance that potentially affects the fauna living on the plateau. It can, however, not directly be measured or observed and separated from icebergs disturbance. Although, the BTM classifies the central part of the plateau as “flat plateau”, the “local ridges on broad flats” and “local depressions” reflect the fine-scale structure of habitat distribution (Fig. 2) seen in the seabed images. Accordingly, in the sheltered depressions, the seabed is covered by abundant IRD often in the form of boulder and gravel pavements. On the ridges and in less sheltered areas, consolidated sediments are exposed (Fig. 3). Towards the rim of the plateau, IRD becomes less abundant and consolidated sediments prevail (Fig. 3). Also there, algae and sessile organisms are limited to sheltered areas. Sessile organisms generally only occur in low abundance and only a small proportion of the available hard substrate is colonised. In the exposed habitats, only mobile fauna can be found.

25 The hill slopes cross several environmental gradients. The presences of algae down to 56 mwd on the northern transect and down to 72 mwd on the southern transect (brown attached to boulders found at 240 mwd must have been displaced by icebergs, Fig. 5a) indicate that the uppermost parts of the slopes are still within the photic zone.

1652

Across the slope, the potential bottom water temperature and salinity are rather constant and only rise by $\sim 0.15^{\circ}\text{C}$ and 0.16 psu.

Geo-morphologically, the hill slopes show even more complex patterns than the plateau. In addition to the general terrace structure (flat areas separated by steeper areas, Fig. 2), small ridges and troughs create a very rugged heterogeneous terrain. These patterns are also reflected in the seabed classification where the slopes are characterised by the seabed classes “broad slopes” and “flat terrain” (Fig. 2). The steps between the terraces are classified as “steep slopes” and on the upper slopes as “escarpment, cliff” (Fig. 2). Some areas with distinct broad scale concave morphology are classified by the BTM as “current scoured depression” (Fig. 2).

Very steep and rugged terrain just below the rim of the plateau, are likely formed by continuous icebergs scouring. By the BTM, these areas with the highest ruggedness are classified as “rock outcrops” (Fig. 2). This classification is in good accordance with the data from the seabed imaged analyses that show common erosion features and escarpments (Fig. 3). Areas classified as “current scoured depression” are another geo-morphological feature on the upper slope are. In this setting they probably also indicate slope failures and small slides. This interpretation is supported by seabed imagery showing slide structures from the upper slopes (Fig. 4c). With these slides limited to the upper slopes, it is probable that they have been triggered by iceberg scouring. At the time of the survey several icebergs were grounded on the upper slope of the hill. In terms of habitat distribution, the entire upper slope can be interpreted as a complex heterogeneous habitat. The delineation of smaller sub-units based on seabed classification and imagery was mere possible as these parameters show no distinct spatial correlation and often vary from image to image which would mean from pixel to pixel in the classification raster. This complexity is also apparent in the correlation of biological and environmental parameters later in the text. On the upper slopes, hard substrate is abundant in the form of consolidated sediment and IRD (Fig. 3). The available hard substrate is, however, not fully colonised.

1653

In comparison with the upper slope, the terrain of the lower slope is less rugged with more gradual changes between “broad slopes” and “flat plains” (Fig. 2). In addition to the dominant classes, long elongated depressions (seabed class “local depression, current scour”) were found on the lower slope, in the north and west of the hill (Fig. 2). They are probably the result of enhanced bottom current activity as they coincide well with the depth range in which current indication have been identified on seabed images (Fig. 3). On the lower slope, the high variability in habitats is not so much the result of rugged and complex terrain but of varying abundance of hard substrate. Hard substrate occurs in the form of IRD and also broken off rocks from the hill. Available hard substrate shows high levels of colonisation.

For the entire slope area, it can be said that in all biological parameters, except for those referring to organisms living exclusively on the plateau and the very upper slope (the algae), the slope shows the highest biological heterogeneity within and between taxa as well as within and between transects. With minor exceptions and with the background of the taxa being generally present in the area: all combinations of taxa can be encountered everywhere.

Although geo-morphologically distinguishable from the background shelf setting (the maximal spatial extent of the hill is delimited by the “broad slope” class), no sedimentological differences can be identified between the hill foot and the background setting. Both settings are characterised by bioturbated soft sediments. Hard substrate only occurs in the form of IRD. Predicted by the BTM and supported by the seabed images, rock outcrops and escarpments are absent. Small areas of “current scoured depressions” are supported by scoured IRD in the vicinity (Figs. 2 and 3) indicating that least temporarily enhanced bottom currents in this area. In terms of habitat characterization, the hill foot and the background setting represent a soft bottom habitat typical for the western Weddell Sea shelf (Fillinger et al., 2013; Gutt, 2006). Hard substrate (IRD) is mostly densely colonized and appears to be the limiting factor for the occurrence of sessile epibenthic organisms. The limited availability of hard substrate is also reflected

1654

The seabed classification results from the BTM are another GIS-derived factor. This factor has only been used in the single-photograph-approach as the data represent non-continuous classes. It does not explain any of the biological patterns well. This means that, according to the applied statistical methods, for the distribution of the epibenthos at the Nachtigaller Hill the three-dimensional small-scale bottom morphology and resulting other potential drivers (e.g. small-scale current regimes) appear not to play an important role. The statistical approach to merge all stations in one data set indicates the search for more general correlations between the environment and the epibenthos, rather than local phenomena.

The generally weak correlations between environmental and biological data can have different reasons:

(1) Environmental factors other than those used in this study mainly drive the biological patterns. Sediment and bottom topography is quite well known in this study. The applied methods also provide valuable information on the generally relevant near-bottom current patterns. However, it cannot be excluded that the very obvious morphological structure of the Nachtigaller Hill acts as an obstacle for the currents on an otherwise flat shelf and causes current peculiarities such as turbulences and lee-situations. Finally, possible superimposed tidal effects are not found.

(2) In combination with large-scale effects, small-scale phenomena are of high relevance. The photograph-wise analyses accommodate this option and the number of photographs is generally high enough to decipher small-scale phenomena. However, some of the observed factors (e.g. current ripples, sand, escarpments, striations, current indicators) only occur very rarely (less than 50 of a total of 1730 photographs). Consequently, the sample size of these specific parameters might be too small to discover statistically significant biota-environment relationships.

(3) Computations with 10-binned photographs generally resulted in higher correlations. This indicates that environmental factors affect the benthos on a larger (~100 m) rather than a smaller scale (single photograph). This explanation does not exclude that, for the benthos local (here single photographs) and possible regional factors (here the

1657

entire investigation area) are also relevant. It is plausible that both scales have their specific significance (e.g., current patterns may primarily act on a larger scale while small-scale sediment variations result in local biological patchiness).

(4) The investigated environmental factors are not the main drivers of the biotic patterns. Instead biological characteristics and interactions may play the dominant role in shaping the benthic communities.

5 Conclusions

Even for the complex morphology encountered at the Nachtigaller Hill, the seabed classification calculated by the BTM returned meaningful patterns. The general geomorphological structure of the hill was well captured, while local features were also represented. Solely derived from bathymetry, the BTM represents a strong tool even for the classification of complex terrains. The geomorphology of the Nachtigaller Hill was characterised by complex and rugged terrain resulting in highly structured, complex heterogeneous habitat distribution. This variability was also represented in the species abundances. Hard substrate for sessile epibenthos is abundant at the hill plateau and slope but rare at the hill foot and in the background deep-shelf setting. The distribution patterns of sessile epibenthos were characterised by highly variable small-scale variability rather than broad distribution zones, reflecting the importance of the heterogeneous geomorphology rather than the influence of more continuous environmental parameters such as water depth or water mass. Most likely it reflects the small elevated areas on the hill slope in combination with patchy distributions of hard substrate. In contrast, the less location-dependent mobile fauna showed broader distribution patterns. The statistical correlation between biota and the analysed environmental factors was, however, generally weak.

Acknowledgements. We thank the captain and crew of R/V *Polarstern* as well as the scientific party of cruise ANT XXIX/3 for their excellent support. Special thanks go to Daniel Damaske

1658

and José Bedmar for their help during bathymetric data acquisition and to Alexandra Segelken-Voigt and Oliver Piepenburg for their help with the seabed image analyses.

References

- Absy, J. M., Schröder, M., Muench, R., and Hellmer, H. H.: Early summer thermohaline characteristics and mixing in the Western Weddell Sea, *Deep-Sea Res. Pt. II*, 55, 1117–1131, doi:10.1016/j.dsr2.2007.12.023, 2008.
- Arndt, J. E., Schenke, H.-W., Jakobsson, M., Nitsche, F. O., Buys, G., Goleby, B., Rebesco, M., Bohoyo, F., Hong, J., Black, J., Greku, R., Udintsev, G., Barrios, F., Reynoso-Peralta, W., Taisei, M., and Wigley, R.: The International Bathymetric Chart of the Southern Ocean (IBCSO) Version 1.0 – a new bathymetric compilation covering circum-Antarctic waters, *Geophys. Res. Lett.*, 40, 1–7, doi:10.1002/grl.50413, 2013.
- Bertolin, M. L. and Schloss, I. R.: Phytoplankton production after the collapse of the Larsen A Ice Shelf, Antarctica, *Polar Biol.*, 32, 1435–1446, doi:10.1007/s00300-009-0638-x, 2009.
- Burrough, P. A. and McDonell, R. A.: *Principles of Geographical Information Systems*, Oxford University Press, New York, 1998.
- Camerlenghi, A., Domack, E. W., Rebesco, M., Gilbert, R., Ishman, S., Leventer, A., Brachfeld, S., and Drake, A.: Glacial morphology and post-glacial contourites in Northern Prince Gustav Channel (NWWeddell Sea, Antarctica), *Mar. Geophys. Res.*, 22, 417–443, 2001.
- Chen, C.-T. and Millero, F. J.: Speed of sound in seawater at high pressures, *J. Acoust. Soc. Am.*, 62, 1129–1135, 1977.
- Clarke, K. R. and Gorley, R. N.: *PRIMER v6: User Manual/Tutorial*, PRIMER-E Ltd., Plymouth, UK, 2006.
- Cummings, V. J., Thrush, S. F., Chiantore, M., Hewitt, J. E., and Cattaneo-Vietti, R.: Macrobenthic communities of the North-Western Ross Sea shelf: links to depth, sediment characteristics and latitude, *Antarct. Sci.*, 22, 793–804, doi:10.1017/S0954102010000489, 2010.
- Dayton, P. K.: Interdecadal variation in an antarctic sponge and its predators from oceanographic climate shifts, *Science*, 245, 1484–1486, 1989.
- Dayton, P. K.: Polar benthos, in: *Polar Oceanography, Part B: Chemistry, Biology, and Geology*, edited by: Smith, W. O., Academic Press, London, 631–685, 1990.

1659

- Dayton, P. K., Kim, S. J., Shannon C., Oliver, J. S., Hammerstrom, K., Fisher, J. L., O'Connor, K., Barber, J. S., Robilliard, G. A., Barry, J., Thurber, A. R., and Conlan, K.: Recruitment, growth and mortality of an antarctic hexactinellid sponge, *Anoxycalyx joubini*, *PLoS ONE*, 8, e56939, doi:10.1371/journal.pone.0056939, 2013.
- Dolan, M. F. J., Grehan, A. J., Guinan, J. C., and Brown, C.: Modelling the local distribution of cold-water corals in relation to bathymetric variables: adding spatial context to deep-sea video data, *Deep-Sea Res. Pt. I*, 55, 1564–1579, 2008.
- Dorschel, B., Hebbeln, D., Foubert, A. T. G., White, M., and Wheeler, A. J.: Hydrodynamics and cold-water coral facies distribution related to recent sedimentary processes at Galway Mound west of Ireland, *Mar. Geol.*, 244, 184–195, doi:10.1016/j.margeo.2007.06.010, 2007.
- Erdey-Heydorn, M. D.: An ArcGIS seabed characterization toolbox developed for investigating benthic habitats, *Mar. Geod.*, 31, 318–358, doi:10.1080/01490410802466819, 2008.
- Fillinger, L., Janussen, D., Lundälv, T., and Richter, C.: Rapid glass sponge expansion after climate-induced Antarctic ice shelf collapse, *Curr. Biol.*, 23, 1–5, doi:10.1016/j.cub.2013.05.051, 2013.
- Genin, A.: Bio-physical coupling in the formation of zooplankton and fish aggregations over abrupt topographies, *J. Marine Syst.*, 50, 3–20, doi:10.1016/j.jmarsys.2003.10.008, 2004.
- Genin, A., Dayton, P. K., Lonsdale, P. F., and Spiess, F. N.: Corals on seamount peaks provide evidence of current acceleration over deep-sea topography, *Nature*, 322, 59–61, 1986.
- Guinan, J., Grehan, A. J., Dolan, M. F. J., and Brown, C.: Quantifying relationships between video observations of cold-water coral cover and seafloor features in Rockall Trough, west of Ireland, *Mar. Ecol. Prog. Ser.*, 375, 125–138, 2009.
- Guo, Y., Davies, P. A., Cavalletti, A., and Jacobs, P.: Topography and stratification effects on shelf edge flows, *Dynam. Atmos. Oceans*, 31, 73–116, 2000.
- Gutt, J.: Some “driving forces” structuring communities of the sublittoral Antarctic macrobenthos, *Antarct. Sci.*, 12, 297–313, doi:10.1017/S0954102000000365, 2000.
- Gutt, J.: Coexistence of macro-zoobenthic species on the Antarctic shelf: an attempt to link ecological theory and results, *Deep-Sea Res. Pt. II*, 53, 1009–1028, doi:10.1016/j.dsr2.2006.02.012, 2006.
- Gutt, J.: Antarctic macro-zoobenthic communities: a review and an ecological classification, *Antarct. Sci.*, 19, 165–182, doi:10.1017/S0954102007000247, 2007.
- Gutt, J.: The Expedition of the Research Vessel *Polarstern* to the Antarctic in 2013 (ANT-XXIX/3), *Berichte zur Polarforschung und Meeresforschung*, p. 150, 2013.

1660

- Gutt, J., Barratt, I., Domack, E. W., d'Udekem d'Acoz, C., Dimmler, W., Grémare, A., Heilmayer, O., Isla, E., Janussen, D., Jorgensen, E., Kock, K.-H., Lehnert, L. S., López-González, P., Langner, S., Linse, K., Manjón-Cabeza, M. E., Meißner, M., Montiel, A., Raes, M., Robert, H., Rose, A., Schepisi, E. S., Saucède, T., Scheidat, M., Schenke, H.-W., Seiler, J., and Smith, C. R.: Biodiversity change after climate-induced ice-shelf collapse in the Antarctic, *Deep-Sea Res. Pt. II*, 58, 74–83, doi:10.1016/j.dsr2.2010.05.024, 2011.
- Gutt, J., Zurell, D., J., B. T., Cheung, W., Clark, M. S., Convey, P., Danis, B., David, B., De Broyer, C., di Prisco, G., Griffiths, H., Laffont, R., Peck, L. S., Pierrat, B., Riddle, M. J., Saucède, T., Turner, J., Verde, C., Wang, Z., and Grimm, V.: Correlative and dynamic species distribution modelling for ecological predictions in the Antarctic: a cross-disciplinary concept, *Polar Res.*, 31, 11091, doi:10.3402/polar.v31i0.11091, 2012.
- Gutt, J., Barnes, D. K. A., Lockhart, S. J., and van de Putte, A.: Antarctic macrobenthic communities: a compilation of circumpolar information, *Nat. Conserv.*, 4, 1–13, doi:10.3897/natureconservation.4.4499, 2013.
- Jakobsson, M., Cherkis, N., Woodward, J., Macnab, R., and Coakley, B.: New grid of Arctic bathymetry aids scientists and mapmakers, *EOS Transactions*, 81, 89–96, doi:10.1029/00EO00059, 2000.
- Jakobsson, M., Macnab, R., Mayer, L. A., Anderson, R. F., Edwards, M., Hatzky, J., Schenke, H.-W., and Johnson, P.: An improved bathymetric portrayal of the Arctic Ocean: implications for ocean modeling and geological, geophysical and oceanographic analyses, *Geophys. Res. Lett.*, 35, L07602, doi:10.1029/2008GL033520, 2008.
- Jakobsson, M., Mayer, L. A., Coakley, B., Dowdeswell, J. A., Forbes, S., Fridman, B., Hodnesdal, H., Noormets, R., Pedersen, R., Rebecco, M., Schenke, H.-W., Zarayskaya, Y., Accettella, D., Armstrong, A., Anderson, R. M., Bienhoff, P., Camerlenghi, A., Church, I., Edwards, M., Gardner, J. V., Hall, J. K., Hell, B., Hestvik, O. B., Kristoffersen, Y., Marcussen, C., Mohammad, R., Mosher, D., Nghiem, S. V., Pedrosa, M. T., Travaglioni, P. G., and Weatherall, P.: The International Bathymetric Chart of the Arctic Ocean (IBCAO) Version 3.0, *Geophys. Res. Lett.*, 39, L12609, doi:10.1029/2012GL052219, 2012.
- Lavaleyre, M. S. S., Thatje, S., Duineveld, G., and Arntz, W. E.: Pelagic larvae and juveniles of benthic invertebrates in the near-bottom environment, *Berichte zur Polarforschung*, 503, 31–35, 2005.

1661

- Lundblad, E., Wright, D. J., Miller, J., Larkin, E. M., Rinehart, R., Naar, D. F., Donahue, B. T., Anderson, S. M., and Battista, T.: A benthic terrain classification scheme for American Samoa, *Mar. Geod.*, 29, 89–111, doi:10.1080/01490410600738021, 2006.
- Orsi, A. H., Nowlin Jr., W. D., and Whitworth III, T.: On the circulation and stratification of the Weddell Gyre, *Deep-Sea Res. Pt. I*, 40, 169–203, 1993.
- Peck, L. S., Barnes, D. K. A., Cook, A. J., A. H., F., and Clarke, A.: Negative feedback in the cold: ice retreat produces new carbon sinks in Antarctica, *Glob. Change Biol.*, 16, 2614–2623, doi:10.1111/j.1365-2486.2009.02071.x, 2010.
- Piepenburg, D. and Müller, B.: Distribution of epibenthic communities on the Great Meteor Seamount (North-East Atlantic) mirrors pelagic processes, *Arch. Fish. Mar. Res.*, 51, 55–70, 2004.
- Post, A. L., Beaman, R. J., O'Brien, P. E., Eléaume, M., and Riddle, M. J.: Community structure and benthic habitats across the George V Shelf, East Antarctica: trends through space and time, *Deep-Sea Res. Pt. II*, 58, 105–118, doi:10.1016/j.dsr2.2010.05.020, 2011.
- Raguá-Gil, J. M., Gutt, J., Clarke, A., and Arntz, W. E.: Antarctic shallow-water megaepibenthos: shaped by circumpolar dispersion or local conditions?, *Mar. Biol.*, 144, 829–839, doi:10.1007/s00227-003-1269-3, 2004.
- Sañe, E., Isla, E., Bárcena, M. Á., and DeMaster, D. J.: A shift in the biogenic silica of sediment in the Larsen B Continental Shelf, off the Eastern Antarctic Peninsula, resulting from climate change, *PLoS ONE*, 8, e52632, doi:10.1371/journal.pone.0052632, 2013.
- Schmidt, K., Atkinson, A., Steigenberger, S., Fielding, S., Lindsay, M. C. M., Pond, D. W., Talling, G. A., Klevjer, T. A., Allen, C. S., Nicol, S., and Achterberg, E. P.: Seabed foraging by Antarctic krill: implications for stock assessment, benthic-pelagic coupling, and the vertical transfer of iron, *Limnol. Oceanogr.*, 56, 1411–1428, doi:10.4319/lo.2011.56.4.1411, 2011.
- Schröder, M., Hellmer, H. H., and Absy, J. M.: On the near-bottom variability in the Northwestern Weddell Sea, *Deep-Sea Res. Pt. II*, 49, 4767–4790, doi:10.1016/S0967-0645(02)00158-3, 2002.
- Smith, C. R., Mincks, S., and DeMaster, D. J.: A synthesis of benthic-pelagic coupling on the Antarctic shelf: food banks, ecosystem inertia and global climate change, *Deep-Sea Res. Pt. II*, 53, 875–894, doi:10.1016/j.dsr2.2006.02.001, 2006.
- Starmans, A., Gutt, J., and Arntz, W. E.: Mega-epibenthic communities in Arctic and Antarctic shelf areas, *Mar. Biol.*, 135, 269–280, 1999.

1662

- Sugden, D. E.: Arctic and Antarctic: a Modern Geographical Synthesis, Basil Blackwell, Oxford, 1982.
- Sumida, P. Y. G., Bernardino, A. F., Stedall, V. P., Glover, A. G., and Smith, C. R.: Temporal changes in benthic megafaunal abundance and composition across the West Antarctic Peninsula shelf: results from video surveys, *Deep-Sea Res. Pt. II*, 55, 2465–2477, doi:10.1016/j.dsr2.2008.06.006, 2008.
- Weiss, A. D.: Topographic Position and Landforms Analysis, 2001.
- Wienberg, C., Beuck, L., Heidkamp, S., Hebbeln, D., Freiwald, A., Pfannkuche, O., and Monteys, F. X.: Franken mound: facies and biocoenoses on a newly-discovered “carbonate mound” on the Western Rockall Bank, NE Atlantic, *Facies*, 54, 1–24, 2008.
- Wienberg, C., Wintersteller, P., Beuck, L., and Hebbeln, D.: Coral Patch seamount (NE Atlantic) – a sedimentological and megafaunal reconnaissance based on video and hydroacoustic surveys, *Biogeosciences*, 10, 3421–3443, doi:10.5194/bg-10-3421-2013, 2013.
- Williams, I. M. and Leach, J. H. J.: The relationship between depth, substrate and ecology: a drop video study from the Southeastern Australian coast, *Oceanol. Acta*, 22, 651–662, 1999.
- Wilson, M. F. J., O’Connell, B., Brown, C., Guinan, J. C., and Grehan, A. J.: Multiscale terrain analysis of multibeam bathymetry data for habitat mapping on the continental slope, *Mar. Geod.*, 30, 3–35, 2007.
- Wood, J.: LandSerf 2.3.1, 2009a.
- Wood, J.: The LandSerf Manual Version 1.0, 3 December 2009 for LandSerf 2.3.1, p. 213, 2009b.
- Wright, D. J., Lundblad, E. R., Larkin, E. M., Rinehart, R. W., Murphy, J., Cary-Kothera, L., and Draganov, K.: ArcGIS Benthic Terrain Modeler [a collection of tools used with bathymetric data sets to examine the deepwater benthic environment], Oregon State University, Davey Jones’ Locker Seafloor Mapping/Marine GIS Laboratory and NOAA Coastal Services Center, 2005.

1663

Table 1. Seabed classification catalogue modified after Erdey-Heydorn (2008). “100” represents one standard deviation of the standardised BPI.

Class	Zone	Fine BPI		Broad BPI		Slope in degree		Depth in metre	
		Lower	Upper	Lower	Upper	Lower	Upper	Lower	Upper
1	Flat Plains	–100	100	–100	100		5		–60
2	Broad Slopes	–100	100	–100	100	5	10		
3	Steep Slopes	–100	100	–100	100	10			
4	Current Scoured Depressions	–100	100		–100				
5	Scarp, Cliff		–100	–100	100	10			
6	Depression		–100		–100				
7	Crevice, Narrow Gullies over elevated terrain		–100	100					
8	Flat Ridge Tops	–100	100	100					
9	Rock Outcrop High, Narrow Ridge	100		100					
10	Local Ridge, Boulders, Pinnacles in Depression	100			–100				
11	Local Ridge, Boulders, Pinnacles on Broad Flats	100		–100	100		5		
12	Local Ridge, Boulders, Pinnacles on Slopes	100		–100	100	5			
13	Local Depression, Current Scours		–100	–100	100		10		
14	Plateau	–100	100	–100	100		5		–60

1664

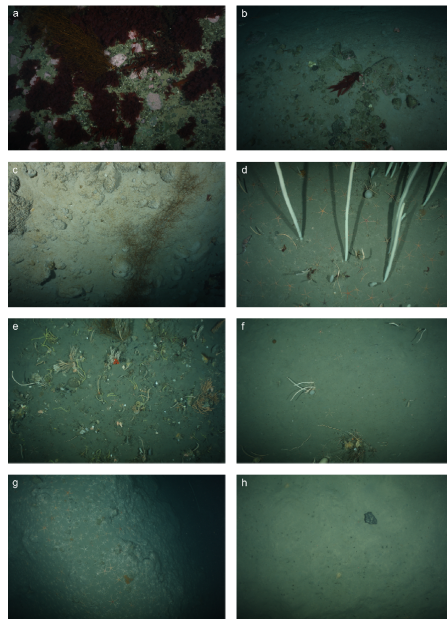


Fig. 4. Selected seabed images of dominant benthic habitats. **(a)** Sheltered area on the plateau (35 m wd), dense boulder and pebble coverage with abundant erect and encrusting red algae. **(b)** Exposed area towards the rim of the plateau (38 m wd). **(c)** Escarpment on the upper slope (56 m wd). **(d–f)** Benthic communities on the slope of the hill in 106 m wd, 308 m wd and 313 m wd. **(g)** Erosional feature with exposed consolidated sediment at 241 m wd with abundant mobile fauna (mostly ophiuroids). **(h)** Background shelf setting at 403 m wd.

1669

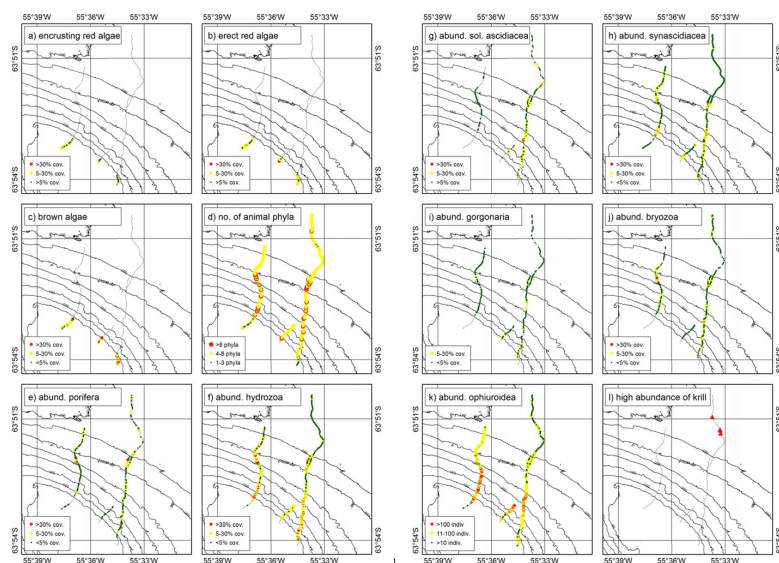


Fig. 5. Abundances of algae **(a–c)** and benthic organism groups **(e–l)** along the OFOS transects. **(d)** Number of animal phyla in each image. This information is an indicator for the distribution of biodiversity on the hill. Abund. = abundance, sol. = solitary.

1670

